Vibratory response of a microperforated plate within an acoustic nonlinear framework

Lucie Gallerand, Mathias Legrand, Thomas Dupont, Raymond Panneton, Philippe Leclaire

25·29 August 2024
inter.noise
NANTES FRANCE

Vibratory response of a microperforated plate within an acoustic nonlinear framework

Lucie Gallerand[1]
Department of Mechanical Engineering, École de technologie supérieure
Montréal, Canada

Mathias Legrand
Department of Mechanical Engineering, McGill University
Montréal, Canada

Thomas Dupont
Department of Mechanical Engineering, École de technologie supérieure
Montréal, Canada

Raymond Panneton
CRASH-UdeS, Department of Mechanical Engineering, Université de Sheerbroke
Sheerbroke, Canada

Philippe Leclaire
DRIVE EA1859, Université de Bourgogne Franche-Comté, ISAT
Nevers, France

ABSTRACT

Microperforated plates (MPP) can add substantial damping in the low-frequency range. MPP are known to dissipate energy through thermo-viscous interactions between shearing adjacent fluid layers near the perforation solid walls. Under linear operating conditions, a previous work carried out by the authors showed that the added damping reaches a maximum at a characteristic frequency which solely depends on the perforation parameters. However, MPP is also suitable in environments subject to high levels of mechanical excitation and, consequently, high fluid velocity within the perforations. Two types of nonlinearities should then be considered: (1) an acoustic nonlinearity induced by high fluid velocity, and (2) a nonlinearity induced by large structural displacements. This work only explores the former. The acoustic nonlinearity is modelled by the Forchheimer resistivity correction, a function of the fluid-solid relative velocity in the perforations, introduced into the equations subsequently solved numerically. Experimental measurements using a laser vibrometer on a perforated cantilever beam validate the proposed model. Results show that, under high excitation levels and at the characteristic frequency, the maximum added damping can reach a maximum, depending on the MPP parameters, at a critical value of the relative fluid-solid velocity.

1. INTRODUCTION

Microperforated plates (MPP) are mainly known for their advantageous acoustic properties and much less for their vibratory properties. When coupled with an air cavity [1], they are efficient

[1]lucie.gallerand.1@ens.etsmtl.ca

acoustic absorbers due to the coupling of reactive and resistive effects of viscothermal nature [2]. They also have the advantage of being able to be manufactured from a multitude of materials.

In a linear acoustic framework, the acoustic absorption of MPPs was studied using models based on i) the work of Champoux and Stinson [3] and the Johnson-Champoux-Allard model applied to perforated plates [4] as well as ii) Kirchhoff's equations [1]. However, MPP are likely to be implemented in hostile environments and it is important to note that these structures are sensitive to the amplitude of excitation [5–7]. Extensions to a nonlinear acoustic regime were carried out using Forchheimer's law and demonstrated maximum acoustic absorption for a critical value of fluid velocity [6].

A previous work by the authors demonstrated that MPPs are good potential candidates for the passive damping of low-frequency vibrations [8]. MPP can dissipate vibrational energy by thermo-viscous interactions taking place in the thermoviscous skin at the level of the solid wall of the perforation. These mechanisms lead to added damping, which reaches a maximum at a *characteristic frequency* of vibration. However, the above study was limited to small perturbations. The present proceeding extends the analysis to a nonlinear framework involving Forchheimer's nonlinear acoustic law.

It is organized as follows: Section 2 briefly recalls the linear *vibration* model and extends it to the nonlinear domain, proposing to use the Forchheimer law. Section 3 presents the analytical results, while Section 4 presents the experimental ones.

2. THEORETICAL BACKGROUND

2.1. Linear model: governing equations

A microperforated plate of dimension $L_x \times L_y \times h$ in the xy plan vibrating under linear operating conditions is considered. The MPP is excited by a punctual driving for $f_{\text{ext}}(\mathbf{x}, t)$ where vector $\mathbf{x} \equiv (x, y)$ are the spatial coordinates. The model developed for porous plates immersed in a fluid of density ρ_f and of bulk modulus K_f [9] is adapted to the context of MPP using an alternative form of Biot's theory. A homogenization procedure is performed, leading to two coupled partial differential equations (PDE) governing the solid motion $w_\text{s}(\mathbf{x}, t)$ and the homogenized relative fluid-solid motion $w(\mathbf{x}, t)$ that verify [8]

$$h(\rho\, \ddot{w}_\text{s}(\mathbf{x}, t) + \rho_\text{f} \ddot{w}(\mathbf{x}, t)) + D(\phi)\nabla^4 w_\text{s}(\mathbf{x}, t) = f_{\text{ext}}(\mathbf{x}, t), \tag{1a}$$

$$\rho_\text{f} \ddot{w}_\text{s}(\mathbf{x}, t) + \frac{\rho_\text{f}\alpha_\infty}{\phi} \ddot{w}(\mathbf{x}, t) + \sigma_0\, \dot{w}(\mathbf{x}, t) + K_\text{f}\nabla^2 w_\text{s}(\mathbf{x}, t) = 0. \tag{1b}$$

Equation (1a) captures the elastic response of the plate and Equation (1b) characterizes the dynamic of a virtual homogenized fluid plate and captures the elastic coupling between the solid and the surrounding fluid into the perforations. The bending coefficient $D(\phi)$ depends on the perforation ratio ϕ and thus captures the influence of the perforations on the MPP stiffness:

$$D(\phi) = \frac{EC(\phi)h^3}{12(1-\nu^2)} \quad \text{with} \quad C(\phi) = \frac{(1-\phi)^2}{1+(2-3\nu)\phi}, \tag{2}$$

where E is Young's modulus of the non-perforated plate and ν is Poisson's ratio which is assumed to be independent of ϕ. The airflow resistivity and the tortuosity are written in terms of d as

$$\sigma_0(d,\phi) = \frac{32\mu_\text{f}}{\phi d^2} \quad \text{and} \quad \alpha_\infty(d,\phi) = 1 + \frac{2\epsilon(d,\phi)}{h} \tag{3}$$

where μ_f is the constant fluid dynamic viscosity and $\epsilon(d,\phi) = 0.24\sqrt{\pi d^2}(1 - 1.14\sqrt{\phi})$ [4] is a correction factor used to reflect the fluid radiation inside the perforations, the distortion of the fluid flow at the perforation orifices and the interactions between flows in the vicinity of perforation orifices. In [8], it was shown that for a mechanically excited MPP, substantial added damping can be

achieved in the low-frequency range. This added damping reaches a maximum at the d-dependent *characteristic frequency*

$$f_c(d) = \frac{32\mu_f}{2\pi\alpha_\infty\rho_f d^2}. \tag{4}$$

The perforation diameter d can then be adjusted to induce maximum damping on a resonance frequency of a plate f_i by forcing f_i to coincide with f_c. In the remainder, this concept of *added damping* is extending to the nonlinear framework by using the Forchheimer law [6, 7].

2.2. Nonlinear MPP model: governing equations

The linear model developed above is only valid for small displacements. If the transverse displacement of the solid increases, the fluid velocity in the microperforations becomes sufficiently high for the resistance and inertia effects occurring in the microperforations to become significant. They are modeled using Forchheimer's law applied to the relative fluid-solid velocity, such as

$$\sigma(\dot{w}(\mathbf{x}), \varepsilon) = \sigma_0(1 + \varepsilon|\dot{w}(\mathbf{x})|) \tag{5}$$

where ε is the Forchheimer parameter obtained by experimental measurement using a high airflow resistivimeter. Inserting Equation (5) into Equation (1) yields the updated system of PDEs

$$h(\rho\ddot{w}_s(\mathbf{x}, t) + \rho_f\ddot{w}(\mathbf{x}, t)) + D(\phi)\nabla^4 w_s(\mathbf{x}, t) = f_{ext}(\mathbf{x}, t), \tag{6a}$$

$$\rho_f\ddot{w}_s(\mathbf{x}, t) + \frac{\rho_f\alpha_\infty}{\phi}\ddot{w}(\mathbf{x}, t) + \sigma_0\dot{w}(\mathbf{x}, t)(1 + |\dot{w}(\mathbf{x}, t)|) + K_f\nabla^2 w_s(\mathbf{x}, t) = 0. \tag{6b}$$

In the experimental setup presented in Section 4, the MPP is subject to a base excitation. It is also proposed in the following to adapt Equation (6) in the case where a harmonic acceleration is imposed at a point of the structure. The total solid and the relative fluid-solid displacement are therefore decomposed into

$$w(\mathbf{x}, t) = w_r(\mathbf{x}, t) + w_e(t) \quad \text{and} \quad w_s(\mathbf{x}, t) = w_{s_r}(\mathbf{x}, t) + w_e(t) \tag{7}$$

where $w_e(t)$ is the harmonic base acceleration with $\ddot{w}_e(t) = \gamma_e \exp(j\omega t)$ with γ_e, the amplitude of the base acceleration and ω, the corresponding angular forcing frequency. The relative motion of the solid with respect to the base is denoted, $w_{s_r}(\mathbf{x}, t)$ while the displacement relative to the base motion of the fluid-solid relative displacement writes $w_r(\mathbf{x}, t)$. Injecting Equation (7) in Equation (6) leads to

$$h\rho\ddot{w}_{s_r} + h\rho_f\ddot{w}_r + D(\phi)\nabla^4 w_{s_r} = -\ddot{w}_e(h\rho - \phi h\rho_f), \tag{8a}$$

$$\rho_f\ddot{w}_{s_r} + \frac{\rho_f\alpha_\infty}{\phi}\ddot{w}_r + \sigma_0(\dot{w}_r - \phi\dot{w}_e) + \sigma_0\varepsilon(\dot{w}_r - \phi\dot{w}_e)|\dot{w}_r - \phi\dot{w}_e| + K_f\nabla^2 w_{s_r} = -\ddot{w}_e(\rho_f - \rho_f\alpha_\infty). \tag{8b}$$

The relative plate motion as well as the relative virtual fluid plate motion are decomposed using the normal modes of the plate without perforation, $\Psi_i(\mathbf{x})$, that is

$$w_{s_r}(\mathbf{x}, t) = \sum_i^N w_i^{s_r}(t)\Psi_i(\mathbf{x}), \quad \text{and} \quad w_r(\mathbf{x}, t) = \sum_i^N w_i^r(t)\Psi_i(\mathbf{x}) \tag{9}$$

where i is the index of the considering mode and N is the number of dof in the discretization. After space semi-discretization, the system of nonlinear PDE is solved numerically using the harmonic balance method. Details about the numerical resolution procedure are provided in [10].

3. THEORETICAL RESULTS

3.1. MPP forced response

The response of a cantilever microperforated beam of dimension 280 mm × 30 mm × 1 mm, subjected to a base excitation at the point $(0, L_y/2)$, is explored in this section using the previous proposed model. To facilitate comparison between theory and experiment presented in Section 4, the plate is chosen to be longer (along x) than wider (along y). Accordingly, modeshapes along y do not participate in the low-frequency range. The perforation diameter and ratio are set to $d = 2.8\,\text{mm}$ and $\phi = 10\,\%$, respectively. The Forchheimer parameter $\varepsilon = 1.42\,\text{s}\,\text{m}^{-1}$ was experimentally measured. Figure 1 represent the frequency response

$$F_X = \left| \frac{w_{\text{s}_\text{r}}(x_m, L_y/2)}{\gamma_\text{e}} \right| \tag{10}$$

predicted by the model for the MPP at point $(x_m, L_y/2) = (260, 15)$ mm for four values of γ_e. The

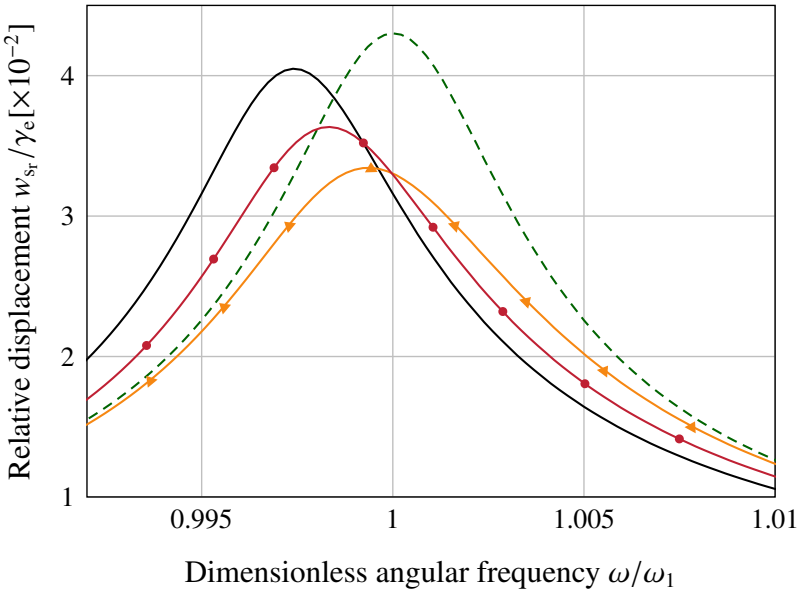

Figure 1: Relative displacement normalized by the base acceleration as a function of the dimensionless angular frequency: (- - -) $\gamma_\text{e} = 0.1\,\text{mm}\,\text{s}^{-2}$, (—▲—) $\gamma_\text{e} = 35\,\text{mm}\,\text{s}^{-2}$, (—●—) $\gamma_\text{e} = 135\,\text{mm}\,\text{s}^{-2}$ and (——) $\gamma_\text{e} = 200\,\text{mm}\,\text{s}^{-2}$.

angular forcing frequency ω is normalized with respect to the first natural frequency ω_1 of the MPP. From Figure 1, two important effects are observed as the amplitude of excitation γ_e increases: i) the stiffness of the system is reduced and ii) damping is effectively increased for the considered MPP. Indeed, the maximum amplitude of displacement decreases and passes through a minimum before increasing with γ_e.

3.2. Sensitivity of MPP vibratory response to nonlinear damping

As previously mentioned, the additional damping in MPP, influenced by viscous dissipation, is determined by the airflow resistivity. In a nonlinear acoustic context, it was noted that the maximum of the absorption coefficient passes though a maximum when the nonlinear normalized resistance

$$R_\text{NL}(d, \dot{w}(x,y,t)) = R_\text{L}(d)(1 + \varepsilon|\dot{w}(x,y,t)|), \quad \text{with} \quad R_\text{L}(d) = \frac{h\sigma_0(\phi, d)}{\rho_\text{f} c_0 \phi^2}, \tag{11}$$

is equal to 1 [6]. The same observations are valid for a vibrating MPP operating under a nonlinear acoustic condition, and the maximum added damping is reached at $R_\text{NL}(d, \dot{w}(x,y,t)) = 1$. Since

$R_{\mathrm{NL}}(d, \dot{w}(x,y,t))$ is an increasing linear function of $\dot{w}(x,y,t)$ three cases are defined from the value of $R_{\mathrm{L}}(d)$, resistance in the normalized linear domain:

$R_{\mathrm{L}} < 1$ the maximum added damping increases with relative fluid-solid velocity until it reaches its maximum, for $R_{\mathrm{NL}}(d, \dot{w}(x,y,t)) = 1$, then decreases with the relative fluid-solid velocity.

$R_{\mathrm{L}} = 1$ the maximum added damping is already at its maximum in the linear regime, so the maximum damping will decrease with the relative fluid-solid velocity.

$R_{\mathrm{L}} > 1$ the maximum added damping will decrease with the relative fluid-solid velocity without ever passing its maximum in the nonlinear regime.

In Figure 1, the perforation diameter and perforation ratio are chosen so that $R_{\mathrm{L}} < 1$. Analytical results can be analyzed using nonlinear normalized resistance. Thus, in Figure 1, $R_{\mathrm{NL}}(d, \dot{w}(x,y,t))$ is less than 1 for $\gamma_{\mathrm{e}} = 0.1\,\mathrm{mm\,s^{-2}}$, greater than 1 for $\gamma_{\mathrm{e}} = 135\,\mathrm{mm\,s^{-2}}$ and $200\,\mathrm{mm\,s^{-2}}$ and equal to 1 for $\gamma_{\mathrm{e}} = 35\,\mathrm{mm\,s^{-2}}$. The last case represents the limit case for which nonlinear dissipative mechanisms are maximized. The corresponding relative fluid-solid velocity is noted *critical relative velocity* and reads

$$V_{\mathrm{c}} = \frac{I_1^{(3)}}{I_1^{(4)}} \frac{\omega \rho_{\mathrm{f}} \alpha_\infty - \sigma_0 \phi}{\sigma_0 \phi \varepsilon}, \tag{12}$$

where V is the amplitude of the relative fluid-solid velocity and $I_1^{(3)}$ and $I_1^{(4)}$ are spatial integrals related to the beam functions in the spatial projection of the coupled equations for the first linear plate mode. Equation (12) is obtained by solving

$$\frac{\partial \eta_1(\omega, V, \varepsilon)}{\partial V} = 0, \tag{13}$$

where $\eta_1(\omega, V, \varepsilon)$ is the added nonlinear loss factor, achieved by adapting the linear loss factor to a nonlinear setting using Equation (5), yielding

$$\eta_1(\omega, V, \varepsilon) = -\frac{h\omega I_1^{(2)} I_1^{(3)}}{D I_1^{(1)}} \cdot \frac{K_{\mathrm{f}} \phi^2 \rho_{\mathrm{f}} \sigma_0 (I_1^{(3)} + \varepsilon V I_1^{(4)})}{(\alpha_\infty \rho_{\mathrm{f}} \omega I_1^{(3)})^2 + (\sigma_0 (I_1^{(3)} + \varepsilon V I_1^{(4)}))^2}. \tag{14}$$

4. EXPERIMENT

4.1. Experimental set-up

The experimental set-up used to validate the proposed model is presented in Figure 2. An aluminum

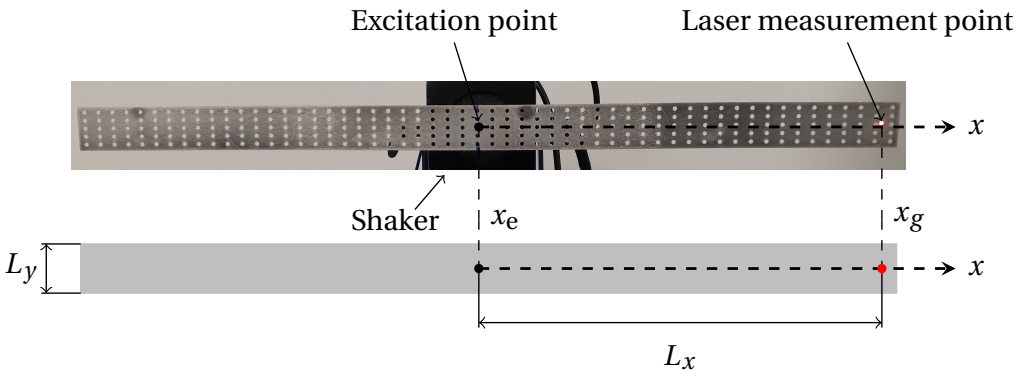

Figure 2: Experimental MPP set-up with the excitation point x_{e} and observation point x_g. The aluminum MPP has dimension 560 mm × 30 mm × 1 mm.

MPP of dimension $L_x = 280\,\mathrm{mm}$, $L_y = 30\,\mathrm{mm}$ and $h = 1\,\mathrm{mm}$ is excited at the point x_{e} and a laser

vibrometer measures the structure velocity at the point x_g. The perforation parameters are set to $d = 2.8\,\text{mm}$ and $\phi = 10\,\%$. In order to reproduce cantilever beam conditions, the MPP is excited at its center by a normal displacement imposed on the z axis [11]. In this configuration, only the even modes of a free beam are participating. The amplitude of the base acceleration γ_e, which acts as a reference force, is maintained constant regardless of ω and the frequency response

$$F_V = \left| \frac{\dot{w}_{s_r}(x_m, L_y/2)}{\dot{w}_{s_r}(x_e, L_y/2)} \right|, \tag{15}$$

is archived.

4.2. Results

The structure is excited by a harmonic base acceleration, $\ddot{w}_e(t) = \gamma_e \cos 2\pi f_e$, sweeping the forcing frequency f_e around the first MPP resonance f_1 with a frequency step of 0.1 Hz. In Figure 3, the normalized velocity V_s/V_e is plotted as a function of f_e/f_1, where $f_1 = 9.28\,\text{Hz}$ is the first natural resonance frequency of the MPP, for four values of base acceleration: $\gamma_e = 10$, 45, 60 and $80\,\text{mm}\,\text{s}^{-2}$. The velocities V_s and V_e correspond respectively to the end beam velocity and the base velocity, both measured with the laser vibrometer. Comparisons between the experimental measurement

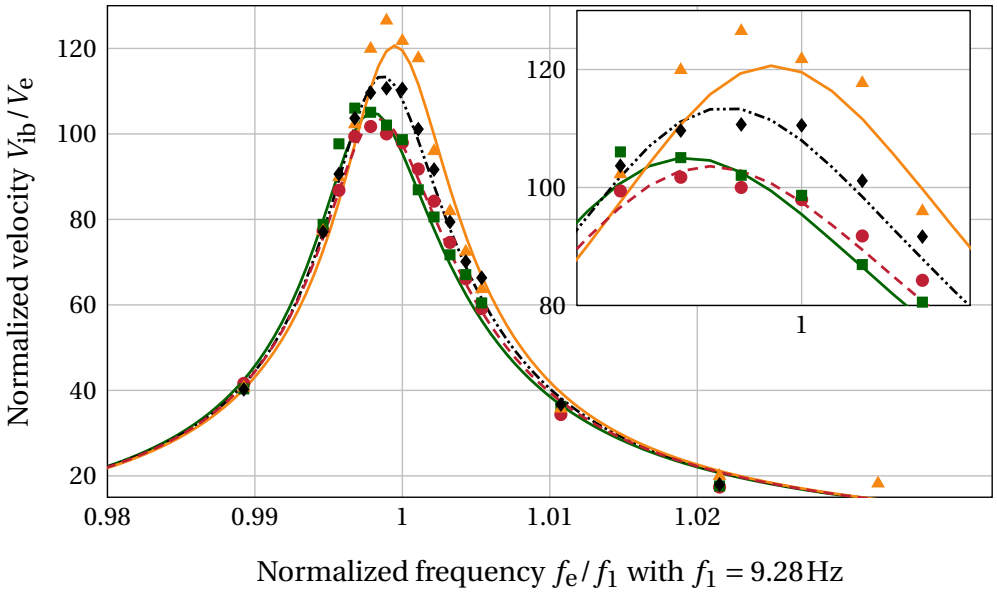

Figure 3: Microperforated plate velocity normalized by base velocity around the first plate resonance f_1 for four base acceleration: (▲) $\gamma_e = 10\,\text{mm}\,\text{s}^{-2}$; (♦) $\gamma_e = 45\,\text{mm}\,\text{s}^{-2}$; (●) $\gamma_e = 60\,\text{mm}\,\text{s}^{-2}$; (■) $\gamma_e = 80\,\text{mm}\,\text{s}^{-2}$. Experimental results shown as markers and corresponding analytical results as solid lines. Experimental results obtained through the set-up presented in Figure 2 and solving Equation (8) with $\varepsilon = 1.42\,\text{s}\,\text{m}^{-1}$.

points and the analytical responses obtained by solving Equation (8) validated the accuracy of the proposed model. In addition, the maximum of the normalized velocity amplitude passes through a minimum that corresponds to the maximum of the added damping. Three steps can be distinguished as excitation amplitude increases : 1) the maximum response amplitude decrease *i.e.* the added damping increase, 2) the maximum response amplitude passes to a minimum *i.e.* the added damping is maximum and the relative fluid-solid velocity is equal to the *critical relative fluid-solid velocity* given in Equation (12), 3) the maximum of response amplitude increase *i.e.* the added damping increase.

5. CONCLUSION

This paper investigated the vibratory response of a fluid-saturated microperforated plate (MPP) within a nonlinear acoustic framework. As an extension of the *vibration* MPP model exposed in [8], an analytical model using Forchheimer's law is proposed and takes the form of two PDEs with an added damping term capturing the resistivity effect induced by acoustic nonlinearities. The analytical model is validated by experimental measurements. This added damping in a nonlinear acoustic context is related to the fluid-structure coupling and therefore to the fluid velocity in the perforations. The results show that the maximum of added damping obtained for $f \approx f_c(d)$ can reach a maximum at a *critical relative velocity* achieved when the normalized nonlinear resistance of the MPP is equal to 1. In order to obtain the maximum added damping in a nonlinear acoustic regime, MPP with a normalized linear resistance of less than 1 is recommended.

REFERENCES

1. D.-Y. Maa. Potential of microperforated panel absorber. *Journal of the Acoustical Society of America*, 104:2861, 1997. [DOI].
2. F.-A. Stremtan, M. Garai, and I. Lupea. Micro-perforated panels and sound absorption. *Applied Mathematics and Mechanics*, 55(3):549–554, 2012.
3. Y. Champoux and M.R. Stinson. On acoustical models for sound propagation in rigid frame porous materials and the influence of shape factors. *Journal of the Acoustical Society of America*, 92:1120–1131, 1992. [DOI], [OA].
4. N. Atalla and F. Sgard. Modeling of perforated plates and screens using rigid frame porous models. *Journal of Sound and Vibration*, 303:195–208, 2007. [DOI], [OA].
5. O. Umnova, K. Attenborough, E. Standley, and A. Cummings. Behavior of rigid-porous layers at high levels of continuous acoustic excitation: Theory and experiment. *The Journal of the Acoustical Society of America*, 114(3), 2003. [DOI], [OA].
6. R. Tayong, T. Dupont, and P. Leclaire. On the variations of acoustic absorption peak with particle velocity in micro-perforated panels at high level of excitation. *The Journal of the Acoustical Society of America*, 127(5):2875–2882, 2010. [DOI], [ARXIV].
7. Z. Laly, N. Atalla, and S-A. Meslioui. Acoustical modeling of micro-perforated panel at high sound pressure levels using equivalent fluid approach. *Journal of Sound and Vibration*, 427:134–158, 2018. [DOI].
8. L. Gallerand, M. Legrand, T. Dupont, and P. Leclaire. Vibration and damping analysis of a thin finite-size microperforated plate. *Journal of Sound and Vibration*, 541:117295, 2022. [DOI], [OA].
9. P. Leclaire, K.V. Horoshenkov, and A. Cummings. Transverse vibration of a thin rectangular porous plate saturated by a fluid. *Journal of Sound and Vibration*, 247(1):1–18, 2001. [DOI], [OA].
10. L. Gallerand, M. Legrand, T. Dupont, R. Panneton, and P. Leclaire. On the vibratory response of a fluid-saturated microperforated plate within an acoustic nonlinear regime. Preprint, 2024 [OA].
11. J.-L. Wojtowicki, L. Jaouen, and R. Panneton. New approach for the measurement of damping properties of materials using the oberst beam. *Review of Scientific Instruments*, 75(8):2569–2574, 2004. [DOI], [OA].